# Dark solitons generated by second-order parametric interactions

K. Hayata and M. Koshiba
*Department of Electronic Engineering, Hokkaido University, Sapporo 060, Japan*
(Received 17 November 1993)

We show that parametric interactions in quadratic nonlinear media can support a novel type of spatial dark soliton. In contrast to the conventional dark soliton in cubic nonlinear media, the most unique feature of the new soliton can be seen in the twin holes in its intensity profile. With a typical nonlinear material, a way to generate the soliton is proposed. A higher-dimensional extension of it is discussed.

PACS number(s): 42.50.Rh, 02.30.Hq, 42.60.Jf, 42.65.Jx

## I. INTRODUCTION

The concept of solitons has now become ubiquitous in modern sciences, and can be found in various branches of physical science [1]. Of these, the type that can be described by the cubic nonlinear Schrödinger equation (NLSE) is regarded as one of the most attractive objects. A representative example of the soliton is found in the laser beam (pulse) propagation in cubic (third-order; $\chi^{(3)}$; Kerr-like) nonlinear media that include fibers [2,3]. As is well known, there exist two kinds of solitons in the canonical (1+1)-dimensional NLSE: bright and dark solitons. Owing to its unique features that cannot be found in the bright soliton, in recent years much attention has been paid to the underlying physics of the dark soliton [4]. In this paper, we present a novel type of dark soliton, taking advantage of mutual supporting assistance resulting from two-wave parametric interaction in quadratic (second-order; $\chi^{(2)}$) nonlinear media. For the new dark soliton we find some remarkable features. Unlike the conventional hyperbolic-tangent-type dark (black) soliton that is based upon the Kerr-type nonlinearity [4], the most unique and fascinating feature of the present $\chi^{(2)}$ dark soliton lies in its topological property in the cross-sectional field profile. As a higher-dimensional solitary-wave (quasisoliton) version of the soliton, an analytical expression for the fundamental-dark-soliton crosses is derived through self-consistent-field (Hartree-like) approximation. With an available nonlinear material, a specific method for generating the new dark soliton is proposed. It is found that the intensity that is needed for exciting it can be lowered optionally by tuning the temperature.

## II. FUNDAMENTAL CONCEPT OF THE DARK SOLITON

As a physical system to support the dark soliton, we consider a phase-matched traveling-wave configuration of optical wave mixing between the fundamental ($\omega$) and the second-harmonic (SH; $2\omega$) frequency components through the second-order nonlinearity of a dielectric medium. From Maxwell's and material equations with a propagation factor, $\exp[in(\beta z-\omega t)]$ ($n=1,2$), being implied, the coupled-wave equations of the slowly varying electric-field amplitudes $A(\omega)$ and $A'(2\omega)$ along the propagation axis $z$ are derivable [5–7]:

$$-i2B\partial_\zeta A=\partial_\xi^2 A+(\varepsilon-B^2)A+2\kappa A^* A' , \tag{1a}$$

$$-i4B\partial_\zeta A'=\partial_\xi^2 A'+4(\varepsilon'-B^2)A'+4\kappa' A^2 , \tag{1b}$$

where $\zeta=k_0 z$ ($k_0$ being the wave number of the fundamental wave in vacuum); $\xi=k_0 x$ ($x$ being a transverse axis); $B=\beta/k_0$ ($\beta$ being a phase constant along the $z$ axis); $\varepsilon$ is the relative permittivity; $\kappa$ represents a relevant component $d_{ij}$ ($i=1,2,3$; $j=1,2,\ldots,6$) that is involved in the second-order nonlinear tensor $[d]$ ($=\frac{1}{2}[\chi^{(2)}]$); and the asterisk denotes complex conjugate. The specific combination of $(A, A';\kappa)$ depends on the crystalline anisotropy as well as the polarization. For instance, for uniaxial crystals [optical ($c$) axis being assumed to align along the $x$ axis] with the class 3 mm of a trigonal system [e.g., ($LiNbO_3$)], we can choose $(A, A';\kappa)=(E_x(e),E_x'(e);d_{33})$, $(E_y(o),E_y'(o);d_{22})$, or $(E_y(o),E_x'(e);d_{31})$, where $o$ ($e$) indicates the ordinary (the extraordinary) wave. Note that in these combinations one need not worry about the spatial walk-off problem [5] since both the waves and the rays are propagating collinearly. (In this context, the method called 90° phase matching [5] may be applicable to the second combination via $d_{22}$.) In this paper the prime (the primeless) indicates the quantity with respect to the SH (the fundamental) frequency component [e.g., $A=A(\omega)$, $A'=A'(2\omega)$; $\varepsilon=\varepsilon(\omega)$, $\varepsilon'=\varepsilon'(2\omega)$]. In the derivation of Eqs. (1) we have confined ourselves to the parametrically coupled dichromatic beams in a transparent medium; effects due to absorptions will be mentioned below (see Fig. 2 and brief discussion in Sec. III). Note that the permutation symmetry [5] requires that $\kappa=\kappa'$.

Imposing the stationarity $\partial_\zeta\equiv 0$ reduces Eqs. (1) to the form

$$d_\xi^2 A+(\varepsilon-B^2)A+2\kappa A^* A'=0 , \tag{2a}$$

$$d_\xi^2 A'+4(\varepsilon'-B^2)A'+4\kappa A^2=0 . \tag{2b}$$

As an ansatz that satisfies the asymptotic behavior, $A(\xi)\neq 0$, $A'(\xi)\neq 0$, and $d_\xi A=d_\xi A'\to 0$, as $\xi\to\pm\infty$, we set

$$A(\xi)=A_0[1-\gamma\,\mathrm{sech}^2(\alpha\xi)] , \tag{3a}$$

 

$$A'(\xi)=A'_0[1-\gamma\,\mathrm{sech}^2(\alpha\xi)]\ , \tag{3b}$$

where $A_0$, $A'_0$, $\alpha$, and $\gamma$ are unknown real constants to be determined below. On substitution of Eqs. (3) into Eqs. (2), solely for $\gamma=\frac{3}{2}$, one can obtain the consistent relations

$$\varepsilon-B^2-4\alpha^2=0\ , \tag{4a}$$

$$4(\varepsilon'-B^2)-4\alpha^2=0\ , \tag{4b}$$

$$2\kappa A_0 A'_0+4\alpha^2 A_0=0\ , \tag{4c}$$

$$4\kappa A_0^2+4\alpha^2 A'_0=0\ . \tag{4d}$$

These are readily solvable for $B$, $\alpha$, $A_0$, and $A'_0$ to yield

$$B=[\varepsilon'+(\Delta\varepsilon/3)]^{1/2}\ , \tag{5a}$$

$$\alpha=(-\Delta\varepsilon/3)^{1/2}\ , \tag{5b}$$

$$A_0=\pm[2^{1/2}/(3|\kappa|)]\Delta\varepsilon\ , \tag{5c}$$

$$A'_0=[2/(3\kappa)]\Delta\varepsilon\ , \tag{5d}$$

with $\Delta\varepsilon\equiv\varepsilon'-\varepsilon$, which must be negative from Eq. (5b). With the spot parameter $\alpha$ being evaluated by Eq. (5b), the full width at half maximum (FWHM) of the global intensity dip can be calculated by the relation FWHM equal to $2.914/(k_0\alpha)$, which is found to be 2.4 times larger than that of the bright soliton in quadratic nonlinear media [7].

The result presented above indicates that Eqs. (3) with $\gamma=\frac{3}{2}$ are a dark-type solitary-wave solution of the physical system under consideration. To verify that this wave has really a solitonic feature, we have carried out numerical stability analyses of the evolution equations, Eqs. (1), using an extended version of the finite-element beam propagation method [8]. A typical result of the axial beam evolution during $2\times10^5\lambda$ ($\lambda$ being the fundamental wavelength in vacuum) propagation is shown in Fig. 1.

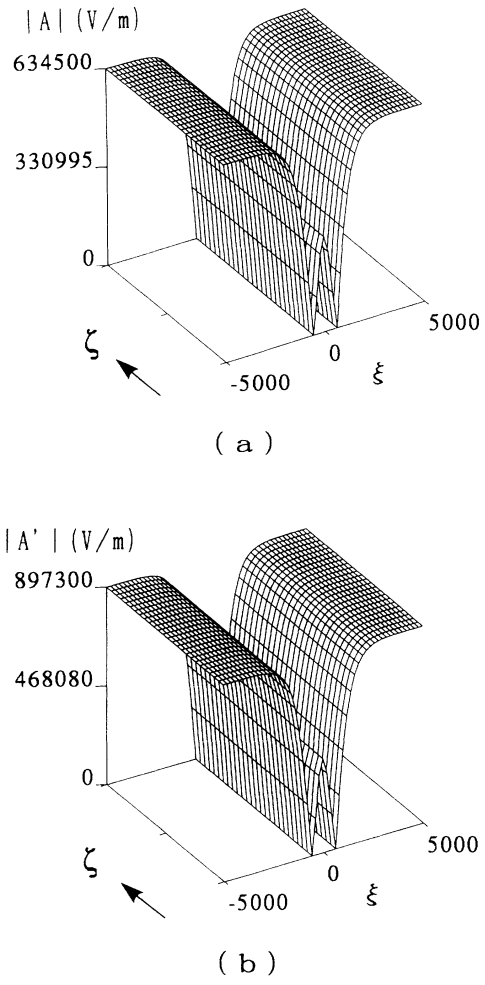


FIG. 1. Bird's-eye view that shows evolution of the parametrically excited dark soliton along the propagation (the $\zeta$) axis ($\zeta=k_0z$, $\xi=k_0x$). (a) Fundamental wave ($\omega$) component, (b) second-harmonic wave ($2\omega$) component. The total propagation distance attains $2\times10^5\lambda$, where $\lambda$ is the fundamental wavelength in vacuum (i.e., $\lambda=2\pi/k_0$). Parametric interaction via $d_{31}$ is considered for $LiNbO_3$. To examine the solitonic feature the medium is assumed to be lossless. The ordinate of (a) plots $|A|=|E_y|$ (ordinary wave), whereas that of (b) plots $|A'|=|E'_x|$ (extraordinary wave), where the single crystallographic (c) axis is set to align along the $x$ axis.

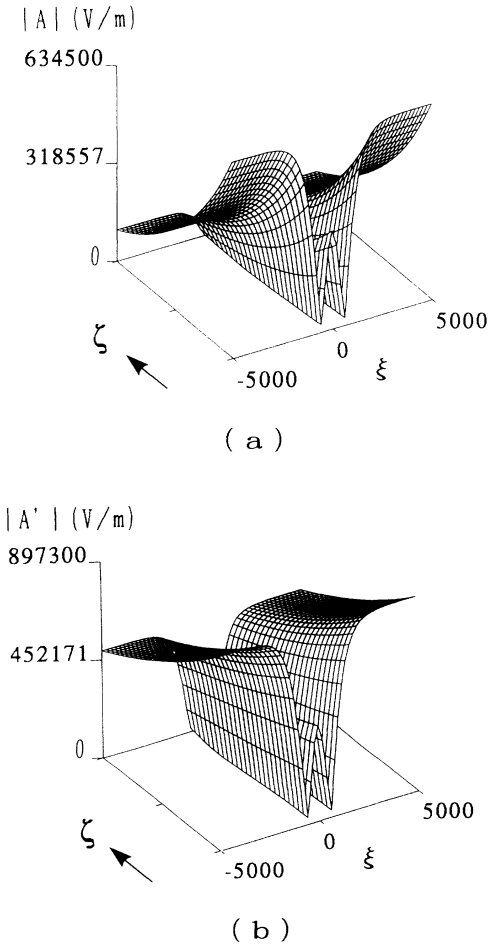


FIG. 2. Same as Fig. 1 but dissipations (one- and two-photon absorptions of $LiNbO_3$) included. Loss parameters used in the simulation have been extracted from Ref. [11], which are given in the text.

The validity of this methodology was fully ensured through extensive applications to stability analyses of solitary waves in Kerr-like media [8,9]. With this method, one first inputs on a computer the solitary wave into a nonlinear medium ($LiNbO_3$) and traces the subsequent variation of the input field during propagation over sufficiently long distances. If the input solution were stable, it would maintain its initial shape after propagation. Through careful analyses we have confirmed that despite a numerical noise that may perturb the signal after the long-distance propagation, the solitary-wave solution we have derived above is stable against propagation (Fig. 1). To check the effect due to a perturbation, similar calculations have been made by including dissipations (one- and two-photon absorptions of $LiNbO_3$). The simulated result is plotted in Fig. 2. The data of the absorption constants have been extracted from Ref. [11], and are given with the description in the subsequent section. Although the amplitude decreases after the long-distance propagation, as in conventional optical solitons in a cubic nonlinear medium with loss [4], the evolution is found to be quasiadiabatic. Numerical results simulated with amplitudes not exactly equal to the values of Eqs. (5c) and (5d) have shown quasistationary propagation provided that the deviation is roughly within 10%. This property is consistent with that of the conventional $\chi^{(3)}$-based dark soliton, which was found to be quite stable against perturbations [4]. All these results verify that Eqs. (1) have a dark-soliton solution. Note that as obvious from Eq. (5c), there exist two modes: $A_0 A_0' > 0$ and $A_0 A_0' < 0$.

## III. NUMERICAL RESULTS AND DISCUSSION

The profiles of the amplitudes and the intensities of the present soliton are sketched in Fig. 3, wherein a unique topological structure is seen, i.e., the transverse phase is reversed at the two sites, $\xi_{\pm} = \pm 0.6585/\alpha$. As depicted in Fig. 3(b), these null points form a local hole doublet in the intensity profile, which propagates independently because of the stationary (the eigenfield) nature of the fundamental soliton. The normalized spacing $\sigma$ between the two valleys is given by the relation $\sigma = \xi_+ - \xi_- = 1.317/\alpha$, which is 45% of the normalized FWHM ($=2.914/\alpha$). The FWHM of each individual hole is estimated to be $0.6597/\alpha$. It should be emphasized here that this noninteracting behavior of the holes is quite unique, and indeed in sharp contrast with the repulsive force acting during the copropagation of two closely spaced dark solitons in Kerr nonlinear media [10]. From Eq. (5b) the spacing is inversely proportional to the square root of the dielectric-constant mismatch $|\Delta\varepsilon|$.

Below we shall explore how to experimentally generate the parametrically excited dark soliton. As obvious from Eqs. (5c) and (5d), to reduce the intensity necessary for forming it, one needs to select a material that exhibits smaller permittivity difference between the two frequency components or larger $\chi^{(2)}$ nonlinearity. Of some candidates we have found nonlinear interaction through $d_{31}$ in $LiNbO_3$ to be the best for this purpose. In this

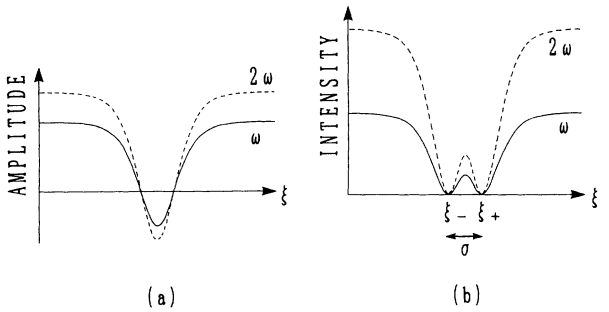


FIG. 3. Transverse profiles of (a) the amplitude and (b) the intensity of the present dark soliton. Twin intensity nulls are seen at $\xi = \xi_+$ and $\xi = \xi_-$; the spacing between them is denoted by $\sigma$.

configuration, the fundamental wave is an ordinary ($o$) wave, whereas the SH wave is an extraordinary ($e$) wave, which corresponds to the third combination mentioned in the preceding section. Taking advantage of the different temperature dependence of the two refractive indices ($n_o, n_e$) [11], one can tune the magnitude of $\Delta\varepsilon$ in an optional fashion. For some typical wavelengths we have examined the variation of $\Delta\varepsilon$ [$=n_e^2(2\omega) - n_o^2(\omega)$] on the temperature. Through the examination we have found that for $\lambda = 1.064$ $\mu$m from a Nd:YAG (where YAG denotes yttrium aluminum garnet) laser, at $t_{cr} \equiv 43.076$ °C, the difference $\Delta\varepsilon$ vanishes completely [7]. To examine the variation of soliton parameters in the vicinity of the critical temperature $t_{cr}$, we plot in Fig. 4 the intensity FWHM, the spacing between the local intensity holes, and the time-averaged intensity [$I \equiv B A_o^2/2$ ($I' \equiv B A_o'^2/2$) for the fundamental (the SH) wave]. The vertical dashed line drawn on Fig. 4 points out $t = t_{cr}$, and all the material data are extracted from Ref. [11] (e.g., $d_{31} = -6$ pm/V). It should be noted that only the lower-half region, $t < t_{cr}$, is allowable, and the region $t > t_{cr}$ is forbidden because therein $\Delta\varepsilon > 0$, which results, from Eq. (5b), in $\alpha$ being imaginary. It can be seen from Fig. 4(a) that the spot size of the soliton decreases with decreasing the temperature, but the rate gets smaller as it

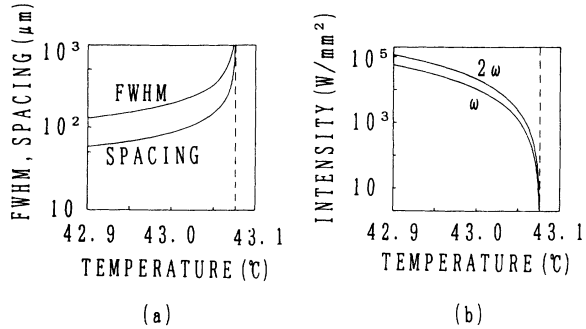


FIG. 4. Temperature dependence of typical soliton parameters in the vicinity of the critical temperature ($\lambda = 1.064$ $\mu$m, $\lambda' = 0.532$ $\mu$m). Parametric interaction via $d_{31}$ is considered for $LiNbO_3$. (a) Intensity FWHM and spacing between holes, and (b) intensity at the plateau. The dashed line points out the critical temperature, $t_{cr} = 43.076$ °C, at which the permittivity mismatch $\Delta\varepsilon$ between the two spectra vanishes.

decreases. The more interesting quantity to observe the soliton is the light intensities that are required to sustain it during propagation. From Fig. 4(b), we find that in the close vicinity of $t_{cr}$ the intensities grow monotonically with decreasing temperature. With a commercially available thermostat, the temperature deviation of 0.01–0.1 °C would be achievable. For instance, at 43.06 °C, one finds from Fig. 4(b), $I=0.6$ kW/mm$^2$, and $I'=1.2$ kW/mm$^2$, which can be realized with the laser under consideration. As in the excitation of the dark soliton in cubic nonlinear media, the use of a suitably designed phase mask [12] allows one to shape the alternating phase profile on the entrance face. Surface damage would be avoidable by adopting a pulsed-mode operation [11]. As has been verified in Fig. 2, effects due to linear absorption will be negligible with propagation distances considerably shorter than the absorption length $L_a$. For $LiNbO_3$, from the data available [11], we estimate $L_a=12.5$ cm for $\lambda=1.064$ $\mu$m, and $L_a'=35.7$ cm for $\lambda'=\frac{1}{2}\lambda=0.532$ $\mu$m. Both the two-photon absorption (TPA) of the visible SH light (TPA coefficient being $2.9\times10^{-9}$ cm/W [11] at 0.532 $\mu$m) and the self-focusing effect (Kerr coefficient being $2.2\times10^{-21}$ m$^2$/V$^2$ [13]) can be ignored at least within the intensity scale shown in Fig. 4(b). Practically, the strict realization of dark soliton will be impossible since infinite power is required for realizing infinite background of the plateau. However, this difficulty will not be crucial because through experiments [14] and numerical simulations [15] of the conventional $\chi^{(3)}$-based dark soliton, it was found that the solitonic feature can be maintained even in a finite background, provided that the plateau is wide enough to ignore the effect of diffraction (dispersion).

## IV. EXTENSION TO HIGHER-DIMENSIONAL SOLITARY-WAVE FIELDS

Finally, we attempt to extend the results presented above to the higher-dimensional solitary waves. For the two-dimensional cross section, Eqs. (2) are replaced with the following equations:

$$(\partial_\xi^2+\partial_\eta^2)A+(\varepsilon-B^2)A+2\kappa A^*A'=0 , \tag{6a}$$

$$(\partial_\xi^2+\partial_\eta^2)A'+4(\varepsilon'-B^2)A'+4\kappa A^2=0 , \tag{6b}$$

where $\eta=k_0y$. Unlike the case of the one-dimensional confinement, for any higher dimension the exact analytical approach is no longer available. In what follows, we shall derive an approximate stationary solution through the use of a self-consistent-field (a Hartree-like) approach [16,17]. With this method the first step is to assume an ansatz in the form of a separation of variables:

$$A(\xi,\eta)=f(\xi)f(\eta) , \tag{7a}$$

$$A'(\xi,\eta)=f'(\xi)f'(\eta) , \tag{7b}$$

where both $f$ and $f'$ are assumed to be real functions that obey the asymptotic behavior of the dark fields.

Substituting Eqs. (7) into Eqs. (6) and applying the Hartree procedure, we obtain a set of the integrodifferential equations,

$$d_v^2f(v)+(\tilde{\varepsilon}-B^2)f(v)+2\tilde{\kappa}f(v)f'(v)=0 , \tag{8a}$$

$$d_v^2f'(v)+4(\tilde{\varepsilon}'-B^2)f'(v)+4\tilde{\kappa}'[f(v)]^2=0 , \tag{8b}$$

with

$$\tilde{\varepsilon}=\varepsilon-\int_{-R}^{R}[d_uf(u)]^2du\Big/\int_{-R}^{R}[f(u)]^2du , \tag{9a}$$

$$\tilde{\kappa}=\kappa\int_{-R}^{R}[f(u)]^2f'(u)du\Big/\int_{-R}^{R}[f(u)]^2du , \tag{9b}$$

$$\tilde{\varepsilon}'=\varepsilon'-\frac{1}{4}\left\{\int_{-R}^{R}[d_uf'(u)]^2du\Big/\int_{-R}^{R}[f'(u)]^2du\right\} , \tag{9c}$$

$$\tilde{\kappa}'=\kappa\int_{-R}^{R}[f(u)]^2f'(u)du\Big/\int_{-R}^{R}[f'(u)]^2du , \tag{9d}$$

for $(u,v)=(\xi,\eta)$, $(\eta,\xi)$. Here $R$ is a positive constant sufficiently larger than the FWHM [$R\gg$(FWHM)], which will be set to be infinite ($R\to\infty$) eventually [17,18]. Note that Eqs. (8) are formally identical to Eqs. (2). Here in the limit of $R\to\infty$, one obtains $\tilde{\varepsilon}\to\varepsilon,\tilde{\varepsilon}'\to\varepsilon'$, $\tilde{\kappa}\to f_0'\kappa$, and $\tilde{\kappa}'\to(f_0^2/f_0')\kappa$, where $f_0\equiv f(\pm\infty)$, $f_0'\equiv f'(\pm\infty)$. Therefore, through the same procedure as used in the one-dimensional case, we can obtain a compact analytical expression of the higher-order fundamental dark fields, Eqs. (7), with

$$f(v)=f_0[1-\tfrac{3}{2}\mathrm{sech}^2(\alpha v)] , \tag{10a}$$

$$f'(v)=f_0'[1-\tfrac{3}{2}\mathrm{sech}^2(\alpha v)] \quad \text{for } v=\xi,\eta , \tag{10b}$$

and with $B$, $\alpha$, $A_0$ ($\equiv f_0^2$), and $A_0'$ ($\equiv f_0'^2$) given by Eqs. (5a), (5b), (5c), and (5d), respectively.

The result of Eqs. (10) shows that in the framework of the Hartree approximation the two dark-soliton components, $f(\xi)$ and $f(\eta)$ [$f'(\xi)$ and $f'(\eta)$] in Eq. (7a) [Eq. (7b)], are supported independently in the nonlinear medium. Note that also for the conventional fundamental dark soliton in cubic nonlinear media, the similar consequence was derived [17]. Therein we showed that this solitary-wave solution can provide a theoretical explanation of a quasisoliton termed a fundamental-dark-soliton cross (FDSC) by Swartzlander *et al.* [12], who demonstrated it experimentally. Here we find that this would be the case as well for the present dark solution for the $\chi^{(2)}$ nonlinearity. A schematic illustration of the FDSC's is depicted in Fig. 5(a); for comparison we show in Fig. 5(b) that of the conventional FDSC in cubic nonlinear media. Obviously, the topological cross section of the present field [Fig. 5(a)] is more complicated than that of the conventional field [Fig. 5(b)]. As in the generation of the FDSC in cubic nonlinear media [12], such a phase distribution will be realizable by placing an optimal phase mask on the entrance face of the nonlinear medium.

Assuming a laser operation with ultrashort pulses, one might expect to obtain the FDSC's in the three-dimensional space-time (i.e., two in space, one in time). Indeed, we have verified that the Hartree approximation for the three-dimensional version of Eqs. (6) leads to the three-dimensional FDSC's, provided that both the group velocities and their dispersions are matchable between the fundamental and the SH pulses. With currently

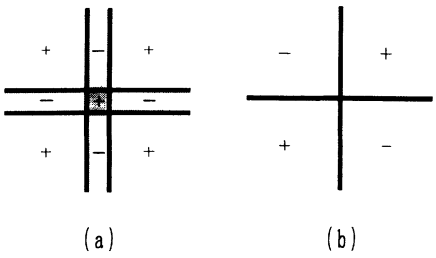


FIG. 5. Schematic of the cross-sectional topology in (a) the present FDSC's that are parametrically generated in quadratic nonlinear media, and in (b) the FDSC that was formed in cubic nonlinear media [12]. Note that in the former there exist quadrupled crosses. In each region on the cross section, the relative phase is marked with a plus or a minus.

available nonlinear materials in mind, this requirement on the time-domain synchronism would be too rigid to be met, especially as the pulse is narrower. In addition, increasing complexities in the three-dimensional (the spatiotemporal) topological profile might render the preparation of a desirable phase configuration extremely difficult.

## V. CONCLUSIONS

We have discovered a novel type of dark soliton, which arises from mutual supporting assistance due to two-wave mixing in quadratic nonlinear media. Subsequently, we have discussed some unique properties of this soliton, proposed a way to generate it, and suggested the possibility of shaping the dark-soliton crosses. Finally, we would like to stress the fact that the results presented herein have close relevance to diverse areas of science, such as, e.g., Fisher-type models in mathematical biology [19] and excitable (activator-inhibitor) systems that can be modeled by Fitzhugh-Nagumo equations [20]. This will ensure that with minor changes the present results are applicable to these problems with different contexts.

## ACKNOWLEDGMENTS

We thank Y. Uehira and H. Higaki for their assistance in the numerical calculation and in surveying the literature, and thank K. Yanagawa for a helpful discussion. This research was partially supported by a Scientific Research Grant-In-Aid from the Ministry of Education, Science and Culture, Japan.

[1] V. G. Makhankov, *Soliton Phenomenology* (Kluwer, Dordrecht, 1990).
[2] A. Hasegawa, *Optical Solitons in Fibers* (Springer-Verlag, Berlin, 1989).
[3] G. P. Agrawal, *Nonlinear Fiber Optics* (Academic, San Diego, 1989).
[4] Yu. S. Kivshar, IEEE J. Quantum Electron. **29**, 250 (1993), and references cited therein.
[5] Y. R. Shen, *The Principles of Nonlinear Optics* (Wiley, New York, 1984).
[6] K. Hayata and M. Koshiba, J. Opt. Soc. Am. B **8**, 449 (1991).
[7] K. Hayata and M. Koshiba, Phys. Rev. Lett. **71**, 3275 (1993); **72**, 178(E) (1994).
[8] K. Hayata, A. Misawa, and M. Koshiba, Trans. IEICE **J73-C-I**, 151 (1990) [Electron. Commun. Jpn. (Part II) **74**, 13 (1991)]; J. Opt. Soc. Am. B **7**, 1772 (1990).
[9] M. Eguchi, K. Hayata, and M. Koshiba, Trans. IEICE **J72-C-I**, 329 (1989) [Electron. Commun. Jpn. (Part II) **73**, 81 (1990)]; **J73-C-I**, **113** (1990) [**73**, 50 (1990)]; K. Hayata, A. Misawa, and M. Koshiba, Trans. IEICE **E73**, 855 (1990); J. Opt. Soc. Am. B **7**, 1268 (1990).
[10] W. Zhao and E. Bourkoff, Opt. Lett. **14**, 1371 (1989).
[11] V. G. Dmitriev, G. G. Gurzadyan, and D. N. Nikogosyan, *Handbook of Nonlinear Optical Crystals* (Springer-Verlag, Berlin, 1991).
[12] G. A. Swartzlander, Jr., D. R. Andersen, J. J. Regan, H. Yin, and A. E. Kaplan, Phys. Rev. Lett. **66**, 1583 (1991); **66**, 3321(E) (1991).
[13] W. L. Smith, in *CRC Handbook of Laser Science and Technology,* edited by M. J. Weber (Chemical Rubber, Boca Raton, 1986), Vol. III.
[14] D. Krökel, N. J. Halas, G. Giuliani, and D. Grischkowsky, Phys. Rev. Lett. **60**, 29 (1988).
[15] W. J. Tomlinson, R. J. Hawkins, A. M. Weiner, J. P. Heritage, and R. N. Thurston, J. Opt. Soc. Am. B **6**, 329 (1989).
[16] K. Hayata and M. Koshiba, Phys. Rev. E **48**, 2312 (1993).
[17] K. Hayata and M. Koshiba (unpublished).
[18] Though such a procedure appears redundant, it will be algebraically necessary when one would like to apply the Hartree ansatz to a multidimensional dark-soliton problem in which the field is transversely unbounded. Note that similar algebra was used in Ref. [17], and its validity was ensured through comparison of the predicted result with the experimental fact. Of course, for bright (bound) solitons, such a trick does not have to be used [7].
[19] J. D. Murray, *Mathematical Biology* (Springer-Verlag, Berlin, 1989).
[20] D. Barkley, M. Kness, and L. S. Tuckerman, Phys. Rev. A **42**, 2489 (1990).

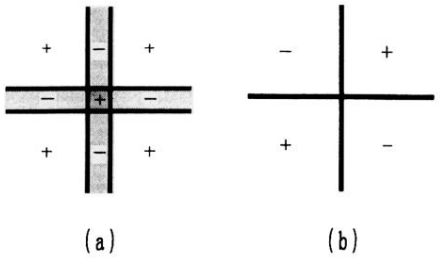


FIG. 5. Schematic of the cross-sectional topology in (a) the present FDSC's that are parametrically generated in quadratic nonlinear media, and in (b) the FDSC that was formed in cubic nonlinear media [12]. Note that in the former there exist quadrupled crosses. In each region on the cross section, the relative phase is marked with a plus or a minus.